

RICE UNIVERSITY

**Microwave spectroscopy on two dimensional  
electron gas**

by

**Jie Zhang**

A RESEARCH PROGRESS REPORT SUBMITTED  
IN PARTIAL FULFILLMENT OF THE  
REQUIREMENTS FOR THE DEGREE  
**Master of Science**

APPROVED, COMMITTEE:

Rui-Rui Du, Chair  
Professor of Physics and Astronomy

Junichiro Kono  
Professor of Electrical and Computer  
Engineering and Physics & Astronomy

Edison Liang  
Professor of Physics and Astronomy

Karl Ecklund Professor of Physics and  
Astronomy

Houston, Texas

August, 2015

# Contents

List of Illustrations	iii
<b>1 Introduction</b>	<b>1</b>
<b>2 Transport behavior of electrons under the illumination of microwave</b>	<b>2</b>
2.1 Shubnikov-de Haas oscillations . . . . .	2
2.2 Microwave induced resistance oscillations . . . . .	3
<b>3 Thermal detection on behavior of electrons under the illumination of microwave</b>	<b>4</b>
3.1 Theoretical support and preparation in 4 K . . . . .	4
3.2 Setup construction . . . . .	6
3.3 Cyclotron resonance pretest . . . . .	7
3.4 Spin resonance on DPPH . . . . .	9
<b>4 Microwave absorption spectroscopy of electrons in 2DEG</b>	<b>11</b>
4.1 Theoretical calculation on resonant frequency . . . . .	11
4.2 Setup construction and calibration . . . . .	12
4.3 Cyclotron resonance pretest . . . . .	13
4.4 Improvement underway . . . . .	14
<b>5 Summary</b>	<b>16</b>

# Illustrations

2.1	Shubnikov-de Haas oscillations . . . . .	3
2.2	Microwave Induced Resistance Oscillations . . . . .	3
3.1	Formation of Landau Levels . . . . .	5
3.2	Non-radiative relaxation . . . . .	5
3.3	Bare chip CR . . . . .	5
3.4	Coupled GR . . . . .	5
3.5	Cernox Thermometer . . . . .	6
3.6	Temperature dependence of the thermometer . . . . .	6
3.7	1266 Epoxy vacuum can . . . . .	6
3.8	Thermal detection setup schema . . . . .	7
3.9	$^3\text{He}$ top-loaded refrigerator coaxial probe . . . . .	7
3.10	CR at 0 dbm 40 GHz . . . . .	8
3.11	Power dependence . . . . .	8
3.12	ESR of DPPH . . . . .	10
3.13	ESR fitting of DPPH . . . . .	10
4.1	Microwave absorption spectroscopy construction . . . . .	12
4.2	setup calibration . . . . .	13
4.3	Polynomial fitting . . . . .	14
4.4	CR pretest . . . . .	14

# Chapter 1

## Introduction

Electron spin resonance (ESR) and cyclotron resonance (CR) are two of the most significant features of electrons under magnetic field. In order to detect the ESR of a single nano-object, a highly sensitive tool is required. So far, the best commercial ESR detector can detect around 1000 spins. We develop an ultra-sensitive calorimeter which is aimed at resolving the ESR of one nano-object. This nano-calorimeter can operate at 300 mK and the precision is improved to tens of micro-Kelvins, thereby increasing the sensitivity to several nano-watts. As a proof of concept, we show that CR can be measured via heat generated by resonant absorption of photons using this setup. An increase in the lattice temperature can be detected when the energy of the incident microwave photons matches the energy difference between adjacent Landau levels, and cannot be detected at other frequencies.

We constructed another setup to investigate edge state transport. Microwave absorption spectroscopy of quantum droplets in a two dimensional electron gas (2DEG) is a powerful tool for investigating the number and velocities of the charge modes. We have sample patterned with multiple circular dots on the order of several microns. It is directly placed onto the meander line superconducting waveguide positioned inside a resonance container. The whole setup is attached to the bottom of a top loaded  $^3\text{He}$  cryostat with base temperature down to 300 mK. This absence of a contact gives this setup an advantage over standard transport measurements and could be generalized to a standard method for probing edge states hosted in other new materials.

## Chapter 2

### Transport behavior of electrons under the illumination of microwave

#### 2.1 Shubnikov-de Haas oscillations

When a magnetic field is applied to an ideal 2DEG, the constant density of states breaks into isolated delta functions with a spacing of  $\hbar\omega_c$ , where  $\omega_c := \frac{eB}{m^*}$  is the cyclotron frequency. In a real 2DEG, these delta functions are broadened (but not shifted) into Lorentzian functions

$$L(E) := \frac{1}{\pi} \frac{\Gamma/2}{(E - E_{LL})^2 + (\Gamma/2)^2} \quad (2.1)$$

due to scattering mechanisms. The peaks  $E_{LL}$  of these Lorentzians are called Landau levels and have a full width at half maximum (FWHM) of  $\Gamma = \hbar/\tau q$  where  $q$  is the quantum lifetime, *i.e.* the mean time between two scattering events. In order to resolve the peak, the magnetic field must be strong enough that  $\hbar\omega_c \gg \Gamma$  or  $\omega_c\tau q \gg 1$ . Heuristically we understand this condition as meaning that an average electron is able to undergo at least one cyclotron orbit without scattering.

The areal density of states in each Landau level denoted by  $n_B := \frac{eB}{h}$  giving a filling factor of  $\nu = \frac{n_{2D}}{n_B} = \frac{h}{eB}n_{2D}$ . Therefore, when the Fermi energy  $E_F$  lies precisely between two separate Landau levels, longitudinal conductance reaches a local minimum and attains a local maximum when  $E_F$  lies on a peak. As the magnetic field pushes the Fermi energy through adjacent Landau levels, the longitudinal resistance  $R_{xx}$  rises and falls, giving rise to the well-known *Shubnikov-de Haas oscillations*

(Figure 2.1).

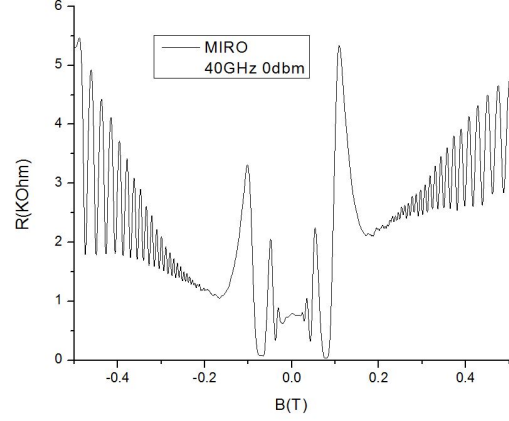
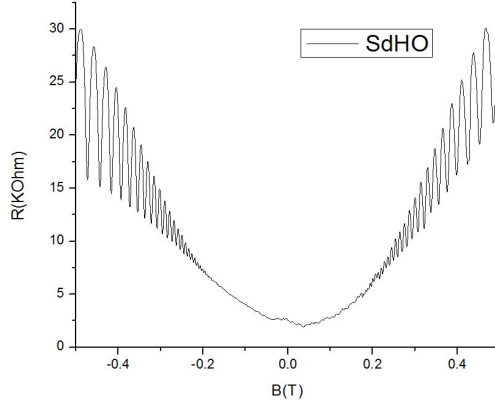


Figure 2.1 : Shubnikov-de Haas oscillations

Figure 2.2 : Microwave Induced Resistance Oscillations

## 2.2 Microwave induced resistance oscillations

When a microwave field is applied, Figure 2.1 changes quite dramatically. Additional maximums appear with different intensity at different peaks which is known as microwave induced resistance oscillations (MIRO), see Figure 2.2. MIRO is fascinating nonequilibrium transport phenomenon found in both n-type and p-type ultrahigh mobility 2D systems.

Theoretical explanations of MIRO involve both a displacement mechanism and an inelastic mechanism [1]. Both these mechanisms modify the scattering of electrons due to microwave assistance. This theory predicts that the photoresistance oscillates as  $\delta R_\omega / R_0 = -2\pi\eta P\lambda^2\epsilon \sin(2\pi\epsilon)$  where  $\eta$  is the dimensionless scattering rate,  $P$  is the dimensionless microwave power,  $\lambda$  is the Dingle factor which is related to the quantum lifetime as well as cyclotron frequency and  $\epsilon := \omega/\omega_c$ .

## Chapter 3

### Thermal detection on behavior of electrons under the illumination of microwave

#### 3.1 Theoretical support and preparation in 4 K

The density of states of a 2DEG forms Landau levels when a magnetic field is applied. However, sweeping either microwave frequency or magnetic field will result in the case where energy of the incident photons is equal to the energy gap of the Landau levels, therefore causing resonance. However, in AlGaAs/GaAs material, electron relaxation can be non-radiative by passing the extra energy to phonons and raising lattice temperature. This temperature change can be measured by a nano-calorimeter. We constructed such a device using a special Cernox thermometer which has a huge resistance difference for a tiny temperature change at low temperature.

This resonance measuring method has been tested in our group with liquid helium for detecting geometric resonance which is the coupling between cyclotron resonance and plasma resonance. On a bare 2DEG chip, cyclotron resonance dips can be resolved clearly.

However, on a patterned sample (with a feature size on the order of  $\mu\text{m}$ ), one can observe two obvious resonances at

$$\omega_{\pm} = \frac{\omega_c}{2} \pm \sqrt{\omega_0^2 + \left(\frac{\omega_c}{2}\right)^2}, \quad (3.1)$$

where  $\omega_0^2 = \frac{N_s e^2}{2m^* \epsilon_{\text{eff}} r}$ , effective mass  $m^* = 0.067m_e$ ,  $\epsilon_{\text{eff}} = 6.5$  and  $r$  is the radius of the dots [2].

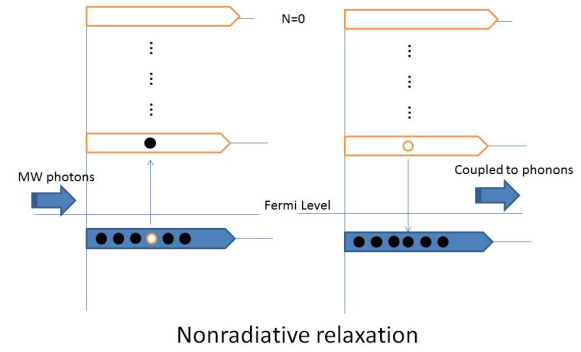
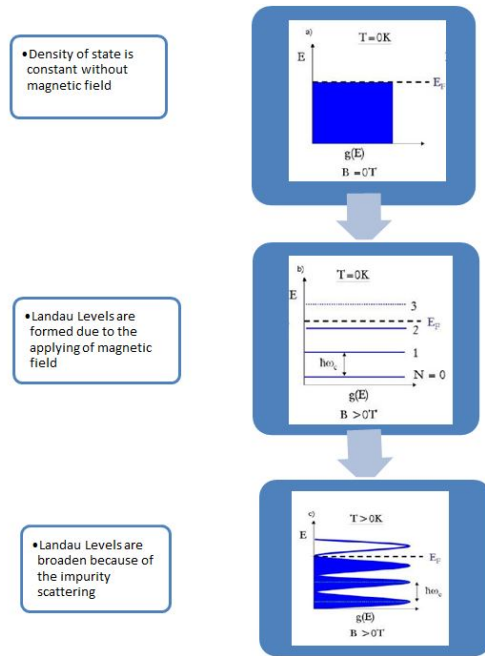


Figure 3.2 : Non-radiative relaxation

Figure 3.1 : Formation of Landau Levels

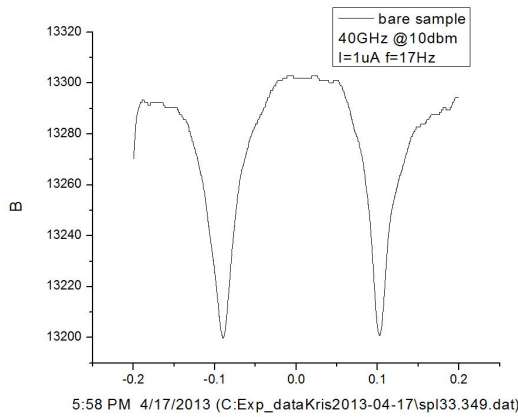


Figure 3.3 : Bare chip CR

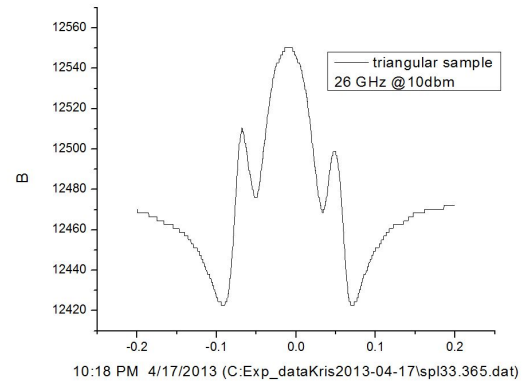


Figure 3.4 : Coupled GR

The boundary plasmon has been eliminated by choosing irregularly shaped samples and the frequency is limited by the size of our waveguide.



### 3.2 Setup construction

In order to improve the sensitivity, we constructed another setup which works in 300 mK due to the fact that the lower the temperature gets, the sharper resistance line the Cernox thermometer's resistance will act (Figure 3.6).



Figure 3.5 : Cernox Thermometer

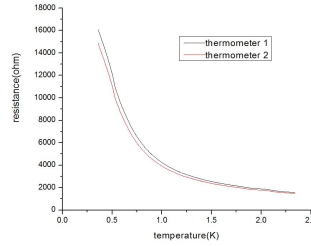


Figure 3.6 : Temperature dependence of the thermometer

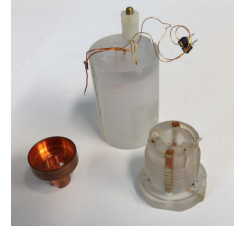


Figure 3.7 : 1266 Epoxy vacuum can

However, going from 4 K to 300 mK is a big leap and there are problems that we have to overcome. The most significant one is sealing in  $^3\text{He}$  liquid environment. Since the heat generated by the non-radiative relaxation is very small, the sample need to be in vacuum to avoid being carried away by massive  $^3\text{He}$  liquid and a high heat conductive media to pass the temperature change to the thermometer. Meanwhile, to keep the temperature around 300 mK, we need something with low heat conductivity to connect the inside setup to outside. In this case, we use thin sapphire crystal as the bridge between sample and thermometer, thin magnin wire for keeping vacuum temperature low. Sealing in  $^3\text{He}$  liquid environment is hard due to the fact that it's molecules are so small that they'll just enter every tiny gap. The way we used to seal is tapping the inner wall of the cap and outer wall of the base therefore compressing the flat surfaces of those two parts to seal. But this is still not enough since the surfaces are polished mechanically only. We dissolve soap in glycerin and then scrubbed it on

the surfaces to fill up any possible tiny gap. Validation of the sealing can only be tested by whether the CR signal is resolved.

The whole vacuum can is immersed in liquid  $^3\text{He}$  in a top-loaded refrigerator. Microwaves are sent through a self-made antenna which is connected to the coaxial cable in the probe (Figure 3.9, Figure 3.8)[3].

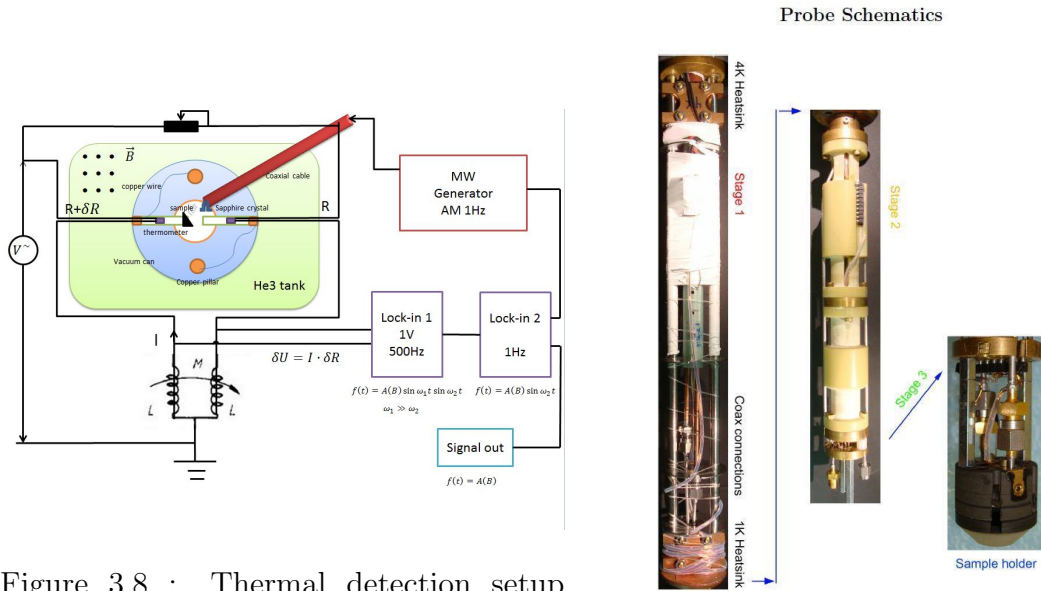


Figure 3.8 : Thermal detection setup schema

Figure D.1: Pictures of the probe stages: 4K, 1K, and the sample holder.

Figure 3.9 :  $^3\text{He}$  top-loaded refrigerator coaxial probe

### 3.3 Cyclotron resonance pretest

We used a differential circuit to filter the background noise and amplitude modulation technique to quench the asymmetry left in the differential geometry. The voltage signal difference from the two arms can be calculated by

$$\frac{|\tilde{E}|}{|\tilde{V}|} = \frac{j\omega_0(M + L)\delta R}{R^2 + 2j\omega_0 RL + \omega_0^2(M^2 - L^2)} \approx \frac{\delta R}{2R} \quad (3.2)$$

This indicates that the output signal  $V_{\text{out}}$  is linearly proportional to the difference between the resistance of those two Cernox thermometers  $\delta R$  which reflects the amount of heat generated by the sample with the illumination of microwave. The differential signal was fed into the first lock-in amplifier the output of which then was fed into the second lock-in amp. The amplitude of the input microwave is modulated internally by the microwave generator according to the frequency of the second lock-in amp which should be much smaller than the rapid oscillating factor of the first lock-in amp. Therefore, after integrating twice, the final output should be a clean response of 2DEG CR signal.

When microwave is applied, obvious resonance peaks appear on each side (see Figure 3.10) and the larger the microwave power gets, the higher the resonance peaks shoot. In Figure 3.11, one can see that the signal can still be resolved even with power as low as -20dbm (0.01 mW). Compared to the setup without these two measuring techniques, sensitivity is at least thirty times higher in terms of input microwave power.

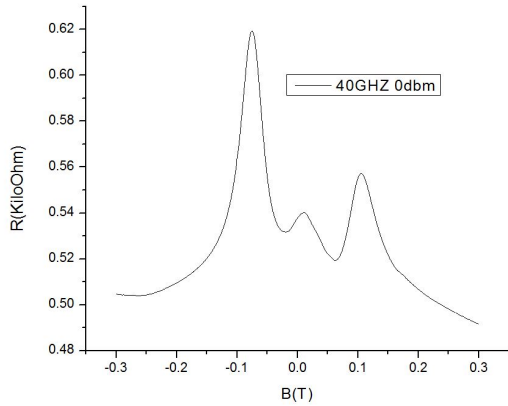


Figure 3.10 : CR at 0 dbm 40 GHz

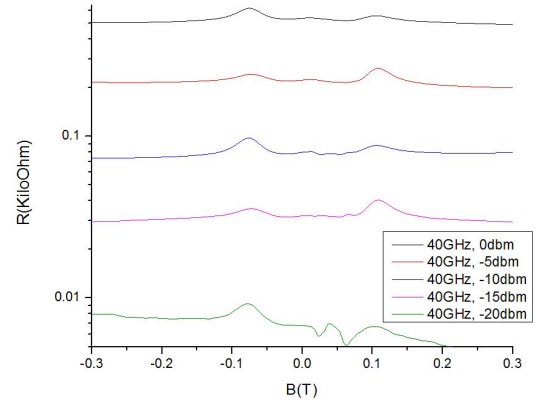


Figure 3.11 : Power dependence

### 3.4 Spin resonance on DPPH

Electron spin resonance (ESR) or electron paramagnetic resonance (EPR) spectroscopy is a technique for studying materials with unpaired electrons using the Zeeman splitting

$$E = m_s g \mu_B B_0 \quad (3.3)$$

where  $g$  is the electron's Landé g-factor and  $\mu_B$  is the Bohr magneton. Therefore, resonance peak happens at

$$\Delta E = g \mu_B B_0 \quad (3.4)$$

The conventional method of measuring ESR is transmission spectroscopy. There are other ways such as magnetic torque detection, optically detected ESR, STM-ESR and resistively detected ESR which measures the longitudinal resistance of 2DEG. Our thermal detection method is another one by measuring the temperature change induced by the non-radiative relaxation of the photon absorption.

DPPH is a common abbreviation for an organic chemical compound 2,2-diphenyl-1-picrylhydrazyl which has two major applications. One is for monitoring chemical reactions involving radicals while the other is determining the position and intensity of ESR signals. In our case, we use dpph to test if ESR signal can be resolved by our setup. Raw data is shown in Figure 3.12 and a clear resonance dip showed up around 1.42 T with a line width of 150 Gauss at the microwave frequency of 40 GHz. Therefore, the g-factor is

$$g = \frac{\hbar \omega}{\mu_B B} = 1.9934 \quad (3.5)$$

while the theoretical value is the free electron  $g = 2.0023$ .

By subtracting the background and fitting with a Lorentzian (Figure 3.13):

$$L(B) = \frac{A}{[1 + (\frac{\mu g \tau}{h})(B - B_r)]^2} \quad (3.6)$$

we have a decoherence time  $\tau = 7.78$  ns which is a reasonable value in our case.

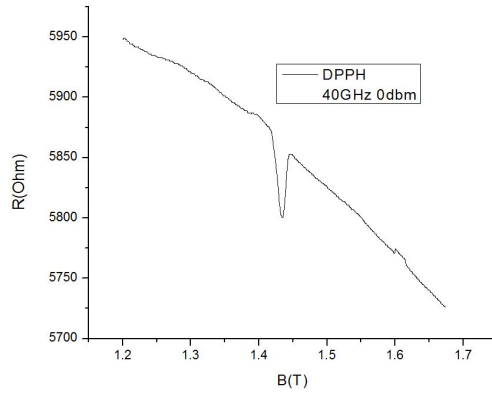


Figure 3.12 : ESR of DPPH

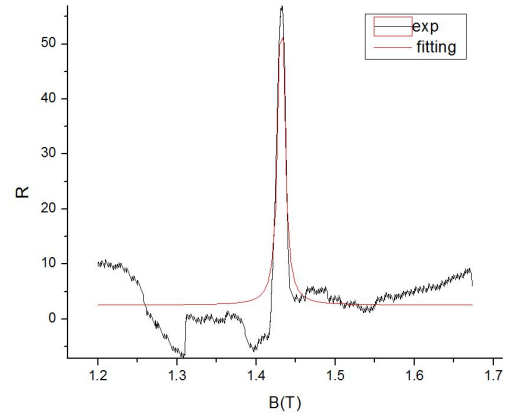


Figure 3.13 : ESR fitting of DPPH

Here, we demonstrated that the nano-calorimeter we constructed has the ability to resolve both CR and ESR signals for those material which has a non-radiative relaxation process.

## Chapter 4

# Microwave absorption spectroscopy of electrons in 2DEG

### 4.1 Theoretical calculation on resonant frequency

This project is aim at investigating the number and velocity of charge modes for edge states on a 2DEG. With its edge being pure one dimensional and dissipationless, it has tremendous potential applications [4]. We patterned high mobility AlGaAs/GaAs wafer ( $n_e \approx 1 \times 10^{11} \text{ cm}^{-2}$ ,  $\mu \approx 15 \times 10^6 \text{ cm}^2/\text{Vs}$ ) with circular discs with a diameter of several microns by lithography. For such a quantum droplet, the minimum energy of the excitations of the edge is  $2\pi\hbar\nu/L$ . The circumference of the droplet is  $L = 2\pi R$  and the velocity of the charge mode  $\nu \approx 1 \times 10^4 \text{ m/s}$ .

To match the microwave energy  $\hbar\omega_M$ , we have

$$\nu = R\omega_M \quad (4.1)$$

Meanwhile, the velocity of electrons going on cyclotron motion under magnetic field is

$$\nu = 2f_c l_B = \frac{2\omega_c}{\pi} l_B \quad (4.2)$$

where  $\omega_c = \frac{eB}{m^*m_0}$  and  $l_B = \sqrt{\frac{\hbar}{eB}} \approx \frac{257}{\sqrt{B}} \text{ \AA}$ . Therefore, for electrons in AlGaAs/GaAs, the resonant frequency is related to the radius of the disc in the following way:

$$R_e = \frac{\omega_x}{\omega_M} \frac{l_B}{\pi} \approx \frac{3.4}{\sqrt{B}} \text{ \mu m/GHz} \quad (4.3)$$

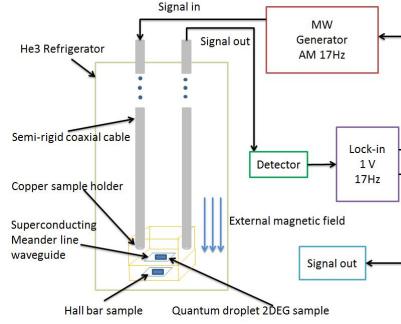


Figure 4.1 : Microwave absorption spectroscopy construction

By sweeping magnetic field or microwave frequency, we should be able to see a resonant peak with a line width related to the distribution of the disc radius.

## 4.2 Setup construction and calibration

We used a co-plane meanderline waveguide ([5]) to hold the patterned sample then placed the waveguide on the top of a broad band sample holder. Electrical connection is done by silver paste. The sample holder is connected to the coaxial cable in the transmission probe by a mini-SMP connector. Again, this whole setup is immersed in  $^3\text{He}$  liquid in a top-loaded cryostat.

We used AM modulation at 17 Hz for measuring except this time, the output signal is the returning microwave intensity. It can be measured by our Schottky diode detector which works in a range of 10 MHz—40 GHz and has a maximum input of 20 dBm. The signal from the detector is a negative voltage which we then feed into our lock-in amp.

We calibrated the system by monitoring the reading of the lock-in amp while sweeping input microwave frequency and power intensity. Figure 4.2 shows the relation between  $V_{\text{out}}$  and  $f_{\text{in}}$  with a constant power of 1 mW. We can see that for small

frequencies (below 12 GHz), it is a linear dependence approximately and there are fluctuations after that.

Figure 4.2 shows how the voltage acts when input power is increased at a sampling rate of 1 GHz. It's reasonable that larger microwave intensity will result in higher voltage reading. And the lower the frequency is, the sharper the slope gets.

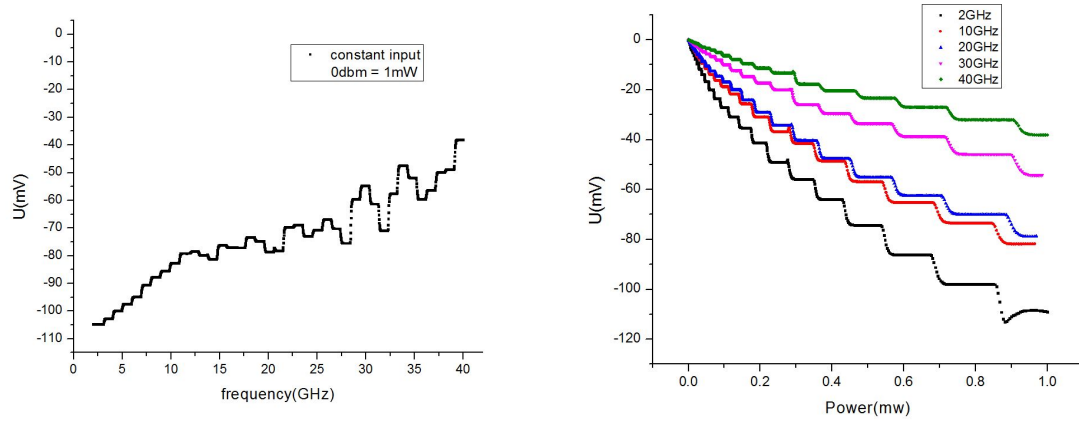


Figure 4.2 : setup calibration

This means our setup works better at lower frequencies. Actually, if we do a polynomial fitting (Figure 4.3) at 2 GHz, the result is very satisfying.

Therefore, it is quite convincing that the negative voltage measured by the detector has a polynomial dependence with the input power intensity.

### 4.3 Cyclotron resonance pretest

CR is a good test for this setup at larger frequencies so that electrons can go at least one circle before any collision and the peaks are separated far enough to resolve. Figure 4.4 shows symmetric CR peaks appear when magnetic field is swept and the signal is higher with larger input power.



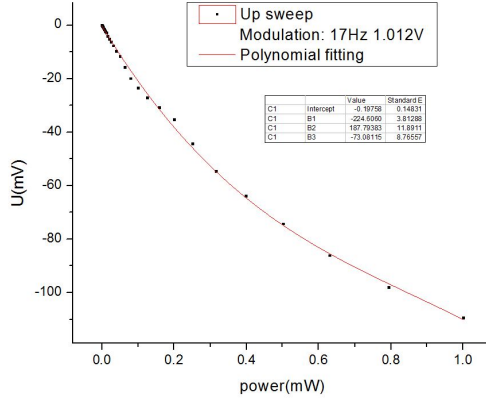


Figure 4.3 : Polynomial fitting

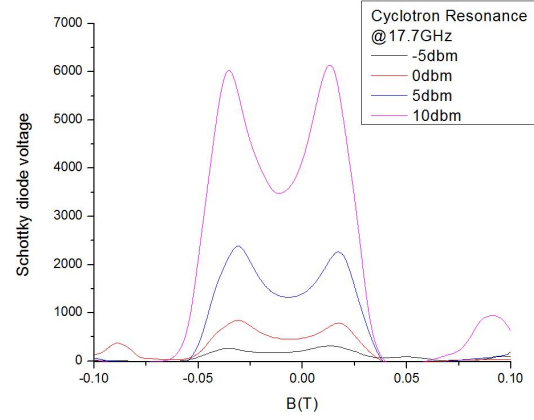


Figure 4.4 : CR pretest

## 4.4 Improvement underway

Though CR can be resolved clearly, we are unable to see authentic repeatable edge state absorption peaks and there are sudden bursts of noise due to reflection and thermal fluctuation. Possible reasons are N-grease being too thick for electric field to probe edge state or even current equipment precision being not high enough to resolve the edge state absorption. However, the most likely problem is the coupling between the microwave and the edge state being not effective enough due to the field polarization.

We came up with a new design to improve the situation using a different configuration. Instead of having the microwave go through a couple of stages attenuated by min-SMP connectors and silver paste, we attach the sample directly to the coaxial cable. We seal the circumference of the sample by soldering indium to the shell of the cable while connect the inner area of the Corbino-like ring to the internal core so that the electromagnetic field is confined in the cable until it reaches the wafer surface which reflects a certain proportion of the energy flow. The returning mi-

crowave is transmitted back through the same cable and measured by the microwave power detector. The way to achieve this is using a directional coupler which has three ports(four ports if it is dual). Directional couplers are passive radio technology devices which couple a define ratio of electromagnetic power in the transmission line to a specific port where the signal is fed to another circuit. By this directional coupling, the returning signal comes out of the coupler without interacting with the original input.

Quantum hall droplets are fabricated within the region between the inner and outer circle of the Corbino-like ring. 2DEG exists inside these droplets, the radius of which must be larger than cyclotron radius but small enough to have an excitation energy within our spectrum(Detail calculation is presented in section 4.1). Polarization of the electromagnetic fields is in the plane perpendicular to the external magnetic field and parallel with the sample surface. Thus, interaction between the electric field and the edge state should be efficient. When the incident microwave photons have energy the same with the first excitation energy of the edge state on the quantum hall droplets, the edge tends to absorb the power causing a decrease in the returning microwave intensity. The key point of this idea is to make sure that the surface of the sample is perfectly perpendicular to the magnetic field in order to avoid any offset in the field calibration for the quantum hall regime thus miss the resonant peak. We manufactured a stage and lay the sample flat on the bottom plane. Then we attach this stage to the probe in a straight line so that the surface of the wafer is in a right angle with the probe which is parallel to the magnetic field in our setup.

We are still considering CR as a pretest measurement since the signal is relatively large and easy to resolve. We regard this setup have higher potential to reveal the resonant peaks for edge state resonance in the quantum hall droplets.

## Chapter 5

### Summary

2D topologically insulating phase in InAs/GaSb is experimentally discovered in our group by Dr.Knez [6] which is an extremely interesting research topic in which the edge of the material is helical because of spin-momentum locking. This phenomenon is protected by time reversal symmetry and consequently the edge conductance is quantized to  $2e^2/h$  even with the presence of nonmagnetic weak disorder. Our goal is eventually being able to detect spin resonance of the edge state electrons in this material where the electron spin absorbs the incident microwave photon energy, flips electron momentum, thus causing a resonant peak in resistivity.

In order to achieve that, we are working on a relatively easier case which is detecting edge states in conventional AlGaAs/GaAs material within the regime of integer quantum hall effect as a pre-step. We fabricated quantum droplets on the wafer by photolithography to form a known shape which is a circle in our case. This edge is pure one dimensional and dissipationless when lies in the quantum hall region which means there is no backscattering. Theoretically, the number and velocity of the modes could be measured directly and different equilibrium regimes can be accessed in the same sample. So far, we've detected various resonance peaks including CR, ESR and GR using microwave with different tools we constructed for different purposes to conduct transport, thermal and absorption measurement. We believe as long as the microwave is effectively coupled to the quantum hall edge, resolving this resonance peak should be achievable.

## Bibliography

- [1] M. A. Zudov, O. A. Mironov, Q. A. Ebner, P. D. Martin, Q. Shi, and D. R. Leadley, “Observation of microwave-induced resistance oscillations in a high-mobility two-dimensional hole gas in a strained ge/sige quantum well,” *Phys. Rev. B*, vol. 89, p. 125401, Mar 2014.
- [2] S. J. Allen, H. L. Störmer, and J. C. M. Hwang, “Dimensional resonance of the two-dimensional electron gas in selectively doped gaas/algaas heterostructures,” *Phys. Rev. B*, vol. 28, pp. 4875–4877, Oct 1983.
- [3] K. Stone, *Millimeter Wave Transmission Spectroscopy of 2D Electron and Hole Systems*. PhD thesis, Rice University, April 2010.
- [4] J. Cano, A. C. Doherty, C. Nayak, and D. J. Reilly, “Microwave absorption by a mesoscopic quantum hall droplet,” *Phys. Rev. B*, vol. 88, p. 165305, Oct 2013.
- [5] C. Clauss, D. Bothner, D. Koelle, R. Kleiner, L. Bogani, M. Scheffler, and M. Dressel, “Broadband electron spin resonance from 500mhz to 40ghz using superconducting coplanar waveguides,” *Applied Physics Letters*, vol. 102, no. 16, pp. –, 2013.
- [6] I. Knez, *Transport Properties of Topological Phases in Broken Gap InAs/GaSb Based Quantum Wells*. PhD thesis, Rice University, March 2012.